Memorandum

Date: May 07, 2011

By: B. M. Wojek
Phone: —
Office: —

To: R. F. Kiefl, M. D. Hossain, J. Baglo

cc: LEM group, E. Morenzoni

On the phase shift observed in LE-μSR Meissner-state measurements

When studying the Meissner effect in superconducting single crystals by means of LE-μSR often a substantial phase shift of the muon-spin-precession signal is observed at high muon implantation energies. This phase shift interferes with the determination of the magnetic penetration depth λ: if the phase is interpreted as purely geometrical parameter it should primarily reflect the detector set-up and the magnitude of the applied field; therefore it should be independent of the sample temperature and also almost independent of the muon implantation energy (for a constant moderator potential). Using recent experimental data on $YBa_2Cu_3O_{6.998}$ single crystals there is a rather large discrepancy between the determined λ if the phase is kept energy-independent [*e.g.* for $\boldsymbol{H} \parallel \boldsymbol{a}$: $\lambda_b(T = 5\ \mathrm{K}) = 96.0(7)$ nm] and if it varies freely [cf. Fig. 1, $\lambda_b(T = 5\ \mathrm{K}) = 82.8(8)$ nm]. Therefore, in order to derive reliable values of the magnetic penetration depth from such measurements the origin of this discrepancy needs to be understood.

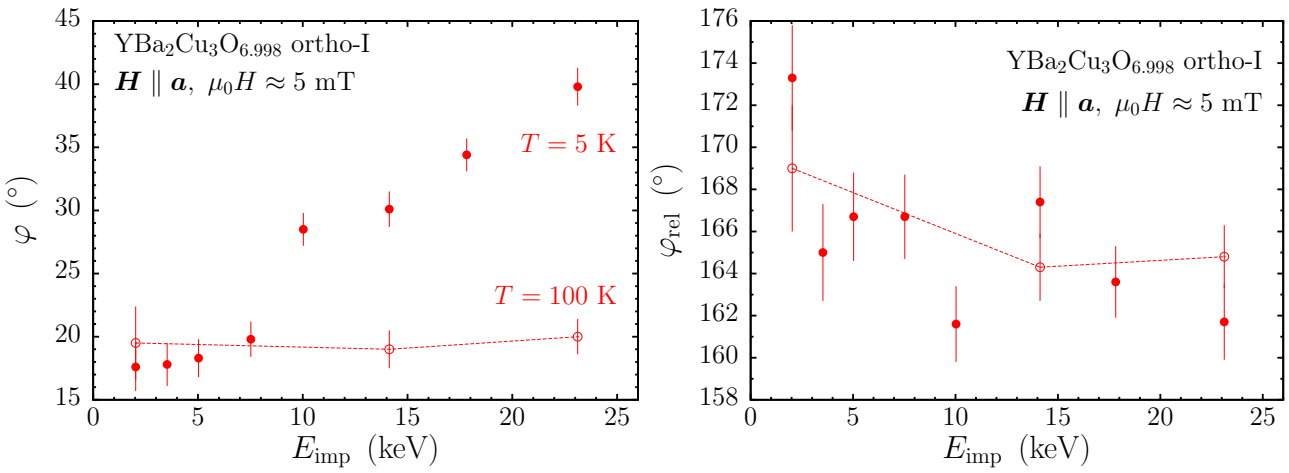

Figure 1: Phases φ and φ_{rel} [see Eq. (4)] of the muon-spin-precession signal in $YBa_2Cu_3O_{6.998}$ in the Meissner state ($T = 5$ K, filled symbols) and above T_c ($T = 100$ K, open symbols) as a function of the muon implantation energy E_{imp}.

In most analyses of LE-μSR data only an average phase, an average "muon implantation time t_0", and a symmetric muon energy spectrum are taken into account. However, this could lead to artifacts in these analyses since the real energy spectrum is asymmetric with a "tail" to lower energies. In order to quantify the resulting effects a set of LE-μSR data has been simulated taking into account the asymmetric energy spectrum and its effects on t_0 and the phase and successively these data have been analyzed using the conventional model employing a symmetric energy spectrum. This procedure shall be described in the following.

Simulation of LE-μSR data

The asymmetric time-of-flight distribution and the corresponding energy spectrum after the trigger detector is obtained from the LEM run `lem08_1351` using the MCP2 detector at the sample position. The moderator high voltage for this run is 15 kV (as it is used for most LE-μSR measurements), yielding a peak energy of about 14.1 keV after the trigger detector. The electrostatic lenses of the muon transport system have been operated at their standard potentials resulting in a "realistic" (with respect to the Meissner-state experiment) time-of-flight distribution; the corresponding "correct" transport-energy spectrum should be obtained from a run where the lenses after the trigger detector are operated at ground potential—for the sake of simplicity, for the present simulations the `lem08_1351` energy spectrum has been shifted to a peak energy of 14.1 keV which already yields a reasonable approximation of this asymmetric spectrum. It is depicted in Fig. 2. Also shown in Fig. 2 is the shift of the muon implantation time t_0 with respect to the "peak implantation time" as a function of the muon energy.

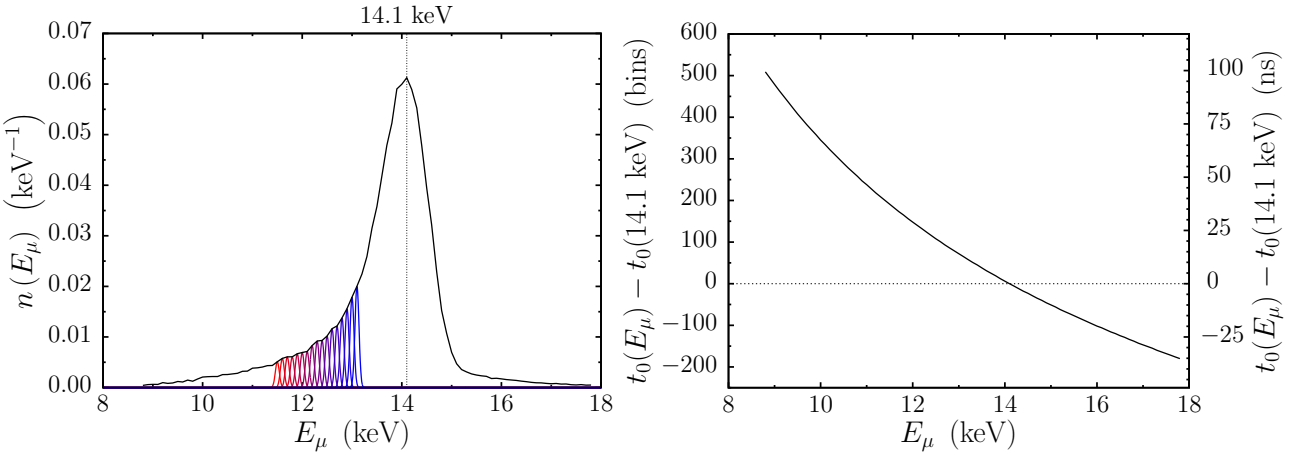

Figure 2: *Left panel:* Approximate muon energy spectrum after the trigger detector. The colored curves exemplary show the sampling of the energy spectrum by symmetric sub-spectra mentioned in the text. *Right panel:* t_0 shift with respect to the implantation time of the muons with an energy at the peak of the energy spectrum. A TDC bin has a width of 0.1953125 ns.

Different effects contribute to the phase of a LEM spin-precession signal (in the B_{parallel} geometry): (i) the spin rotation in the separator (φ_{sep}), (ii) positron absorption effects in the cryostat (φ_{cryo}), and (iii) the spin rotation in the stray field of the sample magnet (φ_{mag}). The total phase then is the sum of this contributions: $\varphi = \varphi_{\mathrm{sep}} + \varphi_{\mathrm{cryo}} + \varphi_{\mathrm{mag}}$. φ_{sep} and φ_{cryo} can be estimated to be about 9° to 11° and 7°, respectively [1]. The phase contribution of the sample magnet is given by

$$\varphi_{\mathrm{mag}} = \gamma_\mu \int \frac{B(z)}{v(z)}\,\mathrm{d}z\,. \tag{1}$$

Neglecting the small effects of the muon acceleration (deceleration) in the sample region this equation can be simplified to

$$\varphi_{\mathrm{mag}} = \frac{\gamma_\mu}{v} \int B(z)\,\mathrm{d}z\,, \tag{2}$$

where $v = \sqrt{2\,E_{\mathrm{trans}}/m_\mu}$ is the classical muon velocity and γ_μ is its gyromagnetic ratio. The magnetic induction along the beam direction $\boldsymbol{z}$ is depicted in Fig. 3. The decay of the induction away from the magnet/sample can be well approximated by

$$B(z) = B_{\mathrm{max}}\,b(z) = B_{\mathrm{max}}\,\left[1 + c_1\,(z/\mathrm{mm})^{c_2}\right] \exp\left[-c_3\,(z/\mathrm{mm})^{c_2}\right]\,, \tag{3}$$

where B_{max} is the induction at the sample position and the constants c_i $(i = 1, 2, 3)$ are given by $\{0.00128906,$ $1.73691, 0.00131476\}$. Using the approximations (2) and (3) φ_{mag} can be readily calculated; figure 3 shows the exemplary energy dependence of φ_{mag} for a sample field of 5 mT.

For the simulation of LE-μSR data the energy spectrum in Fig. 2 is sampled in steps of 100 eV by symmetric sub-spectra with $\sigma_{E_\mu} = 40$ eV as indicated for the energies between 11.5 keV and 13.1 keV in Fig. 2. For each sub-spectrum (shifted by the difference to the final implantation energy) the muon depolarization function in

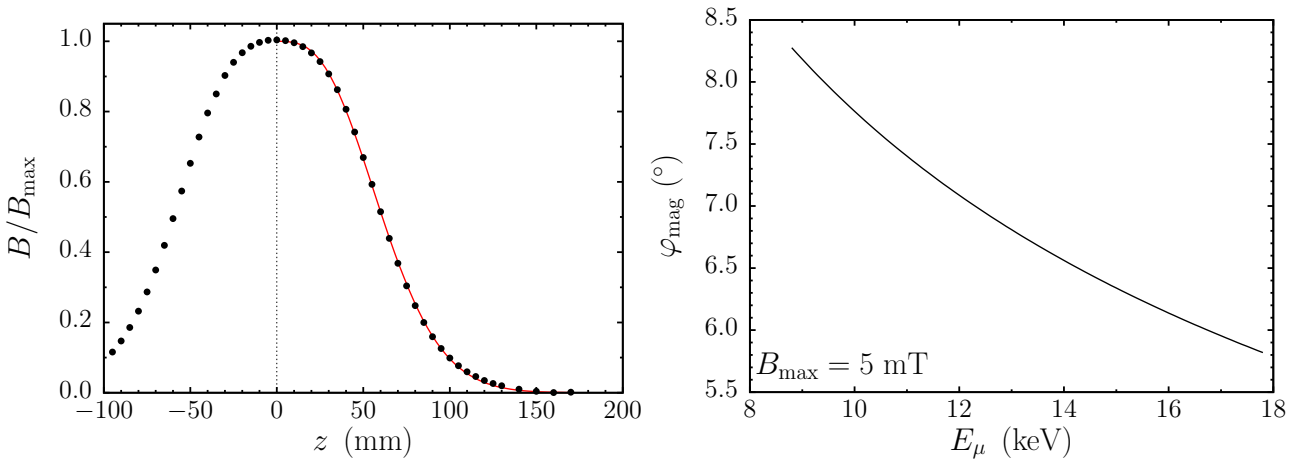

Figure 3: *Left panel:* Normalized magnitude of the magnetic induction in the LEM B_{parallel} geometry as a function of the distance to the sample following the beam direction (adapted from [2]). The red line represents a fit of $b(z)$ introduced in Eq. (3). *Right panel:* Phase shift φ_{mag} picked up by the muons by traversing the magnetic field in front of the sample for $B_{\max} = 5$ mT.

a local superconductor in the Meissner state is calculated [3] and decay histograms are generated according to the respective weight in the spectrum and using the corresponding t_0 as well as phase (cf. Figs. 2 and 3). Finally, all histograms are added in order to obtain a histogram with the full counting statistics (similar to the experiment's). Each generated data file contains two histograms with the only difference that the second histogram has an additional phase shift of 165°, thus mimicking a histogram of the "right detector" of the LEM experiment. Data have been simulated in this way for various muon implantation energies between 2 keV and 25 keV (as typically used in an experiment); for low energies only the part of the muon spectrum which is not reflected in the electrical field in the sample region has been taken into account.
The simulated sample parameters for the "superconducting half-space" are $\lambda = 100$ nm, a dead layer $d = 5$ nm, and different pairs of applied fields $\mu_0 H$ and additional depolarization rates (broadening of the field distributions) σ of $\{2.5\ \mathrm{mT},\ 0.3\ \mu\mathrm{s}^{-1}\}$, $\{5\ \mathrm{mT},\ 0.5\ \mu\mathrm{s}^{-1}\}$, and $\{10\ \mathrm{mT},\ 0.7\ \mu\mathrm{s}^{-1}\}$. Additionally, for each applied magnetic field a set of "reference runs above T_c" ($\lambda = \infty$ or $d = \infty$, $\sigma = 0.1\ \mu\mathrm{s}^{-1}$) has been simulated.
The complete source code of the program used to generate the simulated data files can be found in the LEM subversion repository [4]. Details can be reviewed directly there.

Analysis of the simulated data

The data sets have been analyzed using `musrfit` [5]. Global single-histogram fits for all energies have been employed to determine the relevant parameters "in the Meissner state". In order to model the decay asymmetry the following function has been used:

$$\mathcal{A}(t) = a_{\mathrm{rel}}\, A\, \exp\left(-\frac{\sigma^2 t^2}{2}\right) \int P(B) \cos\left(\gamma_\mu B t + \varphi + \varphi_{\mathrm{rel}}\right) \mathrm{d}B\,, \tag{4}$$

where A is the energy-dependent signal amplitude and $P(B)$ is the modeled static field distribution taking into account the exponential decay of the magnetic induction into the sample (below a dead layer) and the muon implantation profile for a symmetrically broadened energy spectrum. The parameters a_{rel} and φ_{rel} are used to express the signal amplitude and the phase for the "right positron detector" with respect to the "left one". For data in the "left histogram" a_{rel} and φ_{rel} are therefore fixed to values of 1 and 0, respectively.

Before turning to the discussion of the obtained fit parameters it should be noted that the time window for the analysis has to be restricted to times larger than about 100 ns after the "peak implantation time". Figure 4 illustrates that the full count rate is only reached after all muons (also the delayed ones from the tail in the energy spectrum) have been implanted into "the sample". This effect is obscured in real experiments by additional events from muons decaying in flight in front of the sample which contribute substantially to the measured signals around "time-zero".

The analysis returns almost energy-independent broadening parameters σ for the different fields close to the values used for the simulation. Therefore, this parameter will not be discussed further. The energy-dependent

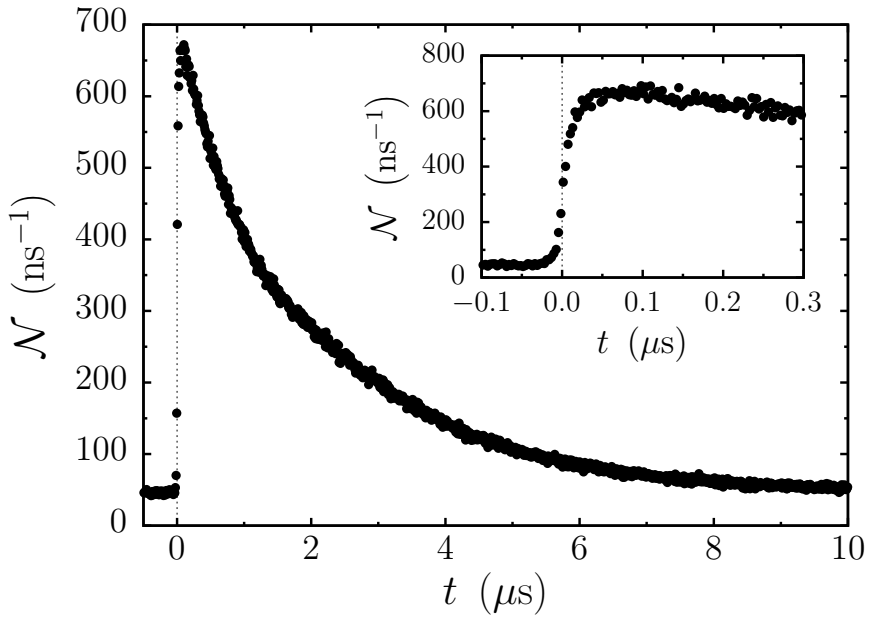

Figure 4: Exemplary simulated "left decay histogram". The time $t = 0$ corresponds to the muon implantation time connected to the peak in the energy spectrum.

phases and signal amplitudes determined by fits of Eq. (4) to the simulated data are depicted in Fig. 5. For the reference data sets these parameters [except A (see below)] are virtually energy-independent for all the employed magnetic fields. The asymmetry A which has been an energy-dependent input parameter for the simulation seems to be determined better the higher is the applied field. The simulated data for the "Meissner state" exhibit a somewhat indecisive behavior. Except a seeming substantial overestimation of the signal amplitude in the "right histogram" at low implantation energies the 2.5 mT data are rather unsuspicious. For the higher fields φ is growing as a function of energy—however, while the effect at 5 mT is even more pronounced in the "right histogram" as evidenced by the simultaneous increase in φ_{rel}, at an applied field of 10 mT the energy dependence of φ_{rel} is opposite to the one of φ, thus rendering the phase in the "right histogram" effectively energy-independent. Additionally, the asymmetry A (at least in the "left histogram") is considerably overestimated in the highest field in almost the full studied energy range.
The "superconducting-state parameters" obtained by this analysis are summarized in Tab. 1. For comparison also the values obtained through global fits with common parameters φ and φ_{rel} for all energies are given. Seemingly, λ and d are determined equally well by both approaches—with the only exception being the 5 mT data for which the phases of both "detectors" (if not common parameters) are increasing as a function of the muon implantation energy and λ is substantially underestimated whereas d is overestimated.

Table 1: Fit parameters obtained through different analyses. In case φ and φ_{rel} are listed explicitly they are common parameters for all energies.

$\mu_0 H$ (mT)	λ (nm)	d (nm)	φ (°)	φ_{rel} (°)
2.5	104.1(1.8)	4.6(0.3)		Fig. 5
2.5	104.4(1.0)	4.6(0.3)	19.3(0.7)	168.9(0.8)
5	93.8(1.9)	8.5(1.0)		Fig. 5
5	100.6(0.8)	6.2(0.9)	24.4(1.0)	164.1(0.7)
10	102.1(1.4)	6.3(0.9)		Fig. 5
10	104.1(0.7)	5.4(0.4)	28.0(0.7)	162.0(0.7)

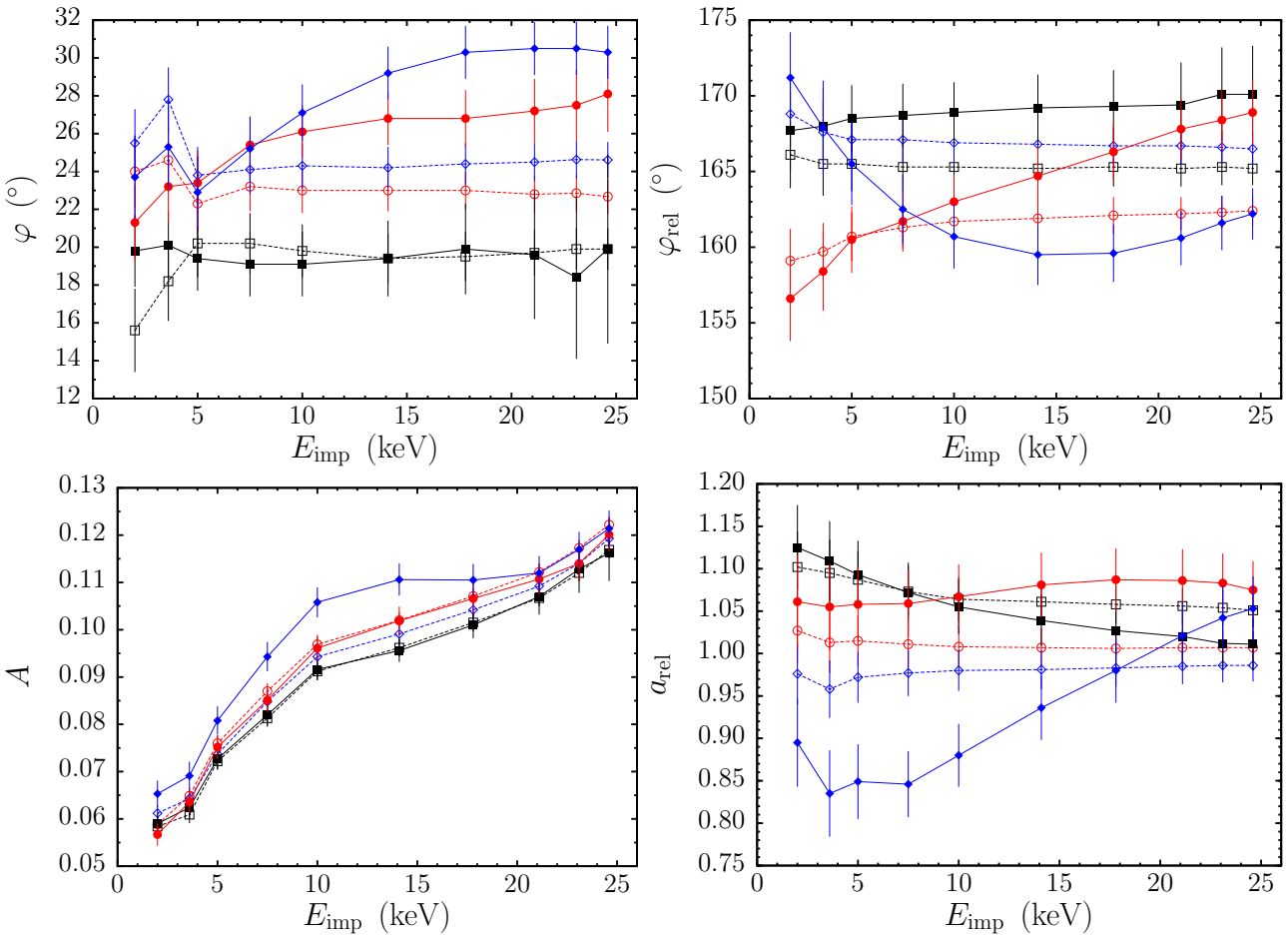

Figure 5: Fit parameters φ, φ_{rel}, A, and a_{rel} introduced in Eq. (4) as a function of the muon implantation energy for the different applied magnetic fields and "temperatures". Black squares, red circles, and blue diamonds correspond to applied fields of 2.5 mT, 5 mT, and 10 mT, respectively. Filled symbols and solid lines represent data "below T_c", open symbols and dashed lines belong to the reference data "above T_c".

Comparison with further experimental data and conclusions

Given the presented data only one firm conclusion can be drawn: ignoring the asymmetric LEM energy spectrum in the data analysis for the studied situation might lead to an artificial phase shift especially at higher implantation energies, however, this effect is too small in order to explain the experimentally observed values presented in Fig. 1.

For further comparison Fig. 6 shows the determined phases for a LE-μSR experiment with a 5-micron thick film of the type-I superconductor indium in the Meissner state. The applied field has been the same as in the $YBa_2Cu_3O_{6.998}$ experiment. The data have been analyzed in the same way as discussed above, except that the static magnetic field distributions are modeled using a Pippard model taking into account nonlocal effects [6]. The magnetic penetration depth is $\lambda_{\mathrm{In}}(T = 2.8\ \mathrm{K}) \approx 30$ nm. The experimental situation is not fully comparable with the simulations, however, the phase shift as a function of the muon implantation energy is of the same order of magnitude as obtained from the above discussed simulations (cf. Fig. 5) and maximally only half of the phase shift depicted in Fig. 1, even though larger fit artifacts can be expected in this case due to the strongly increased diamagnetic field shift in indium compared to $YBa_2Cu_3O_{6.998}$.

Moreover, an independent analysis of the $YBa_2Cu_3O_{6.998}$ data in which the measured field distribution is approximated by the sum of two Gaussian distributions yields roughly the same phase shift as presented in Fig. 1 (where a one-dimensional London model for the Meissner state has been applied to analyze the data). All of this might indicate that the observed energy dependence in φ is not (fully) an artifact—and still needs to be explained *before* λ can be finally determined. Furthermore, the considerable underestimation of λ in one presented case where the phase artificially increases as a function of the muon implantation energy shows that extreme caution has to be exercised when the phase parameters vary freely in the analysis. On the other hand,

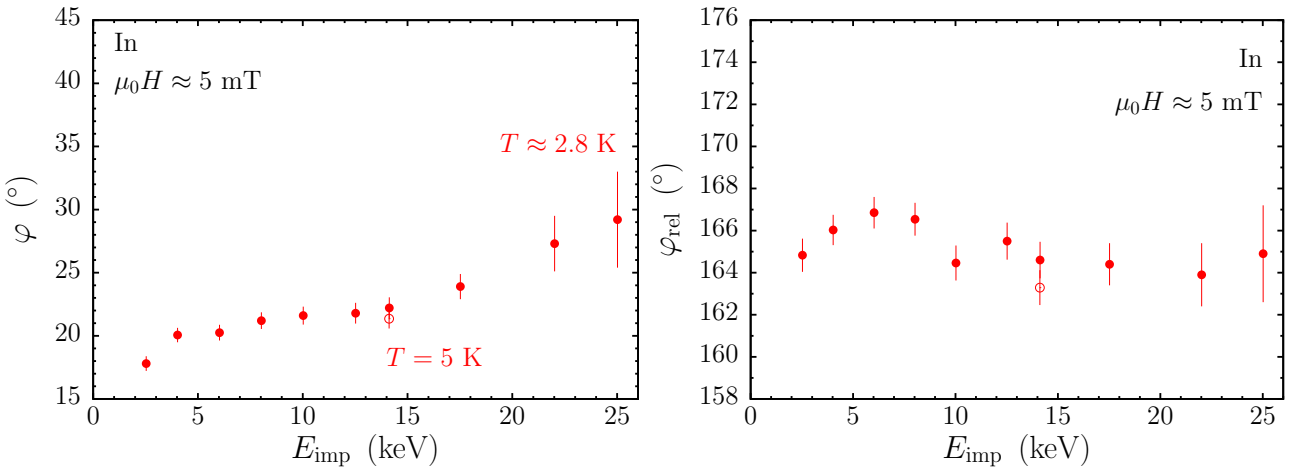

Figure 6: Phases φ and φ_{rel} [see Eq. (4)] of the muon-spin-precession signal in an indium film in the Meissner state ($T \approx 2.8$ K, filled symbols) and above T_{c} ($T = 5$ K, open symbol) as a function of the muon implantation energy E_{imp}. The scales of the axes are identical to the ones in Fig. 1.

keeping the phase as a common parameter for all energies disregards the apparently present phase increase at higher energies and therefore also fails to describe the experimental data accurately.

References

[1] T. Prokscha, *LEM phase considerations*, ELOG:3467, 2007.

[2] S. Populoh, *Examination of the homogeneity of the Birmingham magnet*, 2003.

[3] R. F. Kiefl, M. D. Hossain, B. M. Wojek, S. R. Dunsiger, G. D. Morris, T. Prokscha, Z. Salman, J. Baglo, D. A. Bonn, R. Liang, W. N. Hardy, A. Suter, and E. Morenzoni, *Direct measurement of the London penetration depth in $YBa_2Cu_3O_{6.92}$ using low-energy μSR*, Phys. Rev. B **81** (2010), 180502.

[4] http://savannah.psi.ch/viewcvs/trunk/analysis/musrfit/src/external/libFitPofB/test/simulation?root=nemu%2Flem

[5] A. Suter and B. M. Wojek, to be published. http://lmu.web.psi.ch/facilities/software/musrfit/technical/index.html

[6] A. Suter, E. Morenzoni, N. Garifianov, R. Khasanov, E. Kirk, H. Luetkens, T. Prokscha, and M. Horisberger, *Observation of nonexponential magnetic penetration profiles in the Meissner state: A manifestation of nonlocal effects in superconductors*, Phys. Rev. B **72** (2005), 024506.